Dalton Transactions

Accepted Manuscript

ROYAL SOCIETY OF CHEMISTRY

www.rsc.org/dalton

Synthesis, characterization, and *in vitro* evaluation of new coordination complexes of Platinum(II) and Rhenium(I) with a ligand targeting the translocator protein (TSPO).

Nicola Margiotta,[*,a] *Nunzio Denora,*[b] *Sara Piccinonna,*[a] *Valentino Laquintana,*[b] *Francesco Massimo Lasorsa,*[c] *Massimo Franco,*[b] *and Giovanni Natile*[*, a]

[a] Department of Chemistry, University of Bari "Aldo Moro", via E. Orabona 4, 70125, Bari, Italy;

[b] Department of Pharmacy - Drug Sciences, University of Bari "Aldo Moro", via E. Orabona 4, 70125, Bari, Italy;

[c]CNR Institute of Biomembranes and Bioenergetics, Via Amendola 165/a, 70126, Bari, Italy.

Corresponding Authors

*Phone: +39 080 5442759 (N.M.); +39 080 5442774 (G.N.). E-mail: nicola.margiotta@uniba.it (N.M.); giovanni.natile@uniba.it (G.N.).

Keywords

Platinum, Rhenium, TSPO, bifunctional chelate ligand, heteronuclear complexes.

Abstract

The 18-kDa translocator protein (TSPO) is overexpressed in many types of cancers and is also abundant in activated microglial cells occurring in inflammatory neurodegenerative diseases. The TSPO-selective ligand 2-(8-(2-(bis(pyridin-2-yl)methyl)amino)acetamido)-2-(4-

chlorophenyl)*H*-imidazo[1,2-*a*]pyridin-3-yl)-*N*,*N*dipropylacetamide (CB256), which fulfills the requirements for a bifunctional chelate approach, has been used to synthesize coordination complexes containing either Pt (**1**) or Re (**3**), or both metal ions (**2**) with. The new metal complexes showed a cellular uptake markedly greater than that of the precursor metallic compounds and were also able to induce apoptosis in C6 glioma cells. The good cytotoxicity of the free ligand CB256 towards C6, A2780, and A2780cisR tumor cell lines was attenuated after coordination of the dipicolylamine moiety to Pt while coordination of the imidazopyridine residue to Re reduces the affinity towards TSPO. The results of the present investigation are essential for the design of new imidazopyridine bifunctional chelate ligands targeted to TSPO.

Introduction

The 18-kDa translocator protein (TSPO)[1] is a mitochondrial protein associated with a wide number of biological processes including cell proliferation, apoptosis, steroidogenesis, and immunomodulation.[2] TSPO has become an attractive target for therapeutic and imaging purposes,[3-5] due to its abnormal expression in multiple diseases, including brain, breast, colon, prostate, and ovarian cancers, as well as astrocytomas and hepatocellular and endometrial carcinomas.[6,7] Consequently, TSPO represents an extremely attractive subcellular target to image disease states overexpressing this protein, but also for a selective mitochondrial drug delivery.[8-11] In previous studies we reported on the synthesis of potent and selective imidazopyridine-based TSPO ligands,[12,13] such as [2-(4-chlorophenyl)-8-amino-imidazo[1,2-a]pyridin-3-yl]-*N*,*N*-di-*n*-propylacetamide (CB86),[8] and 2-[6,8-dichloro-2-(1,3-thiazol-2-yl)*H*-imidazo[1,2-*a*]pyridin-3-yl]-*N*,*N*-di-*n*-propylacetamide (TZ6).[14,15] These ligands were used as coordinating moieties for

the preparation of cytostatic platinum species. The platinum complexes *cis*-[$PtX_2(NH_3)$(CB86-*N*)] (X = Cl, I) and *cis*-[$PtCl_2$(TZ6-*N,N*)] (Chart 1) demonstrated to keep the high affinity (nanomolar concentration) and selectivity for TSPO characteristic of the free ligands.[12,13]

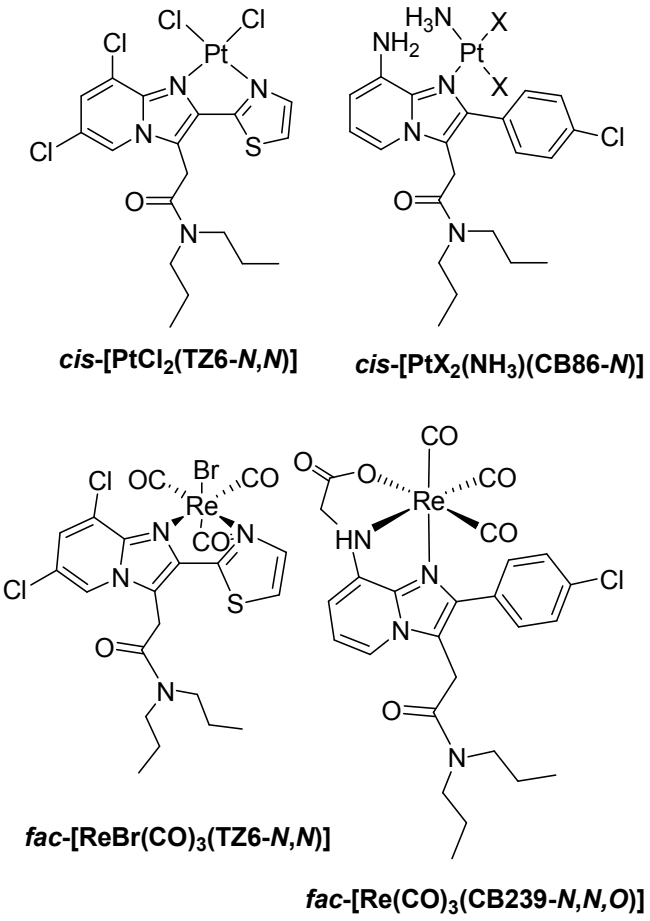

***cis*-[$PtCl_2$(TZ6-*N,N*)]** ***cis*-[$PtX_2(NH_3)$(CB86-*N*)]**

***fac*-[$ReBr(CO)_3$(TZ6-*N,N*)]**

***fac*-[$Re(CO)_3$(CB239-*N,N,O*)]**

Chart 1. Sketches of *cis*-[$PtCl_2$(TZ6-*N,N*)], *cis*-[$PtX_2(NH_3)$(CB86-*N*)] (X = Cl, I), *fac*-[$ReBr(CO)_3$(TZ6-*N,N*)], and *fac*-[$Re(CO)_3$(CB239-*N,N,O*)].

TSPO expression is also increased in activated microglial cells occurring in inflammatory neurodegenerative diseases such as Alzheimer, Parkinson, Huntington, and multiple sclerosis.[16] Therefore, TSPO-targeted metal complexes could be also explored for imaging purposes, especially for the early diagnosis of neurodegenerative diseases.[17]

To this end, we have recently prepared new $^{185/187}$Re complexes (Chart 1) containing the TSPO ligands TZ6 and 2-(2-(4-chlorophenyl)-3-(2-(dipropylamino)-2-oxoethyl)imidazo[1,2-*a*]pyridin-8-yl-amino)acetic acid (CB239). Also these latter complexes, *fac*-[ReBr(CO)$_3$(TZ6-*N,N*)][18] and *fac*-[Re(CO)$_3$(CB239-*N,N,O*)][19] (Chart 1), have been found to be endowed with good affinity for TSPO.

In the compounds so far investigated we used donor atoms already present in the TSPO ligand for anchoring the metal core; a further step would be the use of conjugates in which the targeting ligand is linked with an appropriate chelating system capable to form a strong coordination compound with the radionuclide (^{99m}Tc/$^{186/188}$Re) in a pertinent oxidation state.[20] The use of an appropriate linker could rule out possible interactions between the metal-core and the targeting moiety so to leave unaltered the pharmacokinetic profile of the tracer. Such a strategy is commonly reported as bifunctional chelate (BFC) approach.[21]

To this aim we recently prepared a new TSPO-selective BFC ligand, namely 2-(8-(2-(bis(pyridin-2-yl)methyl)amino)acetamido)-2-(4-chlorophenyl)*H*-imidazo[1,2-*a*]pyridin-3-yl)-*N*,*N*-dipropylacetamide (CB256 in Chart 2).[20] CB256 showed an *in vitro* affinity for TSPO in the submicromolar range and a very high cytotoxicity due to the ability of the dipicolylaminic moiety to coordinate endogenous metal ions and cause single- and double-strand DNA lesions.[20] CB256 showed also the ability to cause collapse of the mitochondrial membrane potential ($\Delta\Psi_m$), inducing mitochondrial and nucleus morphology modifications. The overall features of CB256 resembling those of bleomycin.[22]

In the present investigation we have exploited the coordination potential of CB256 towards Pt^{II} and Re^{I} metal ions (compounds **1**, **2**, and **3** in Chart 2, respectively). The goal was to provide

new compounds that could be used as radiodiagnostic (by substituting γ-emitting ^{99m}Tc for cold $^{185/187}$Re) or radiotherapeutic (by substituting β-emitting $^{188/186}$Re for $^{185/187}$Re).[23,24] In addition, we wanted to assess if the bleomycin-like action of the free ligand CB256 could be substituted by the cytotoxic activity of Pt^{II} coordination compounds, or reduced by the coordination of Re^{I} metal ions. Compound **1** shares great similarity with the antitumor active Hollis type compounds (*cis*-[$PtCl(NH_3)_2$(pyridine)]Cl)[25] or the more recent phenanthriplatin.[26] It is cationic (and as such can take advantage of the organic cation transporters OCT1 and OCT2[27,28] to enter cells) and has only one position available for coordination to DNA. It is worth mentioning that this work represents, to our knowledge, the first study describing a potential selective TSPO theranostic agent characterized by a imidazo[1,2-*a*]pyridine nucleus bearing two metal binding sites.

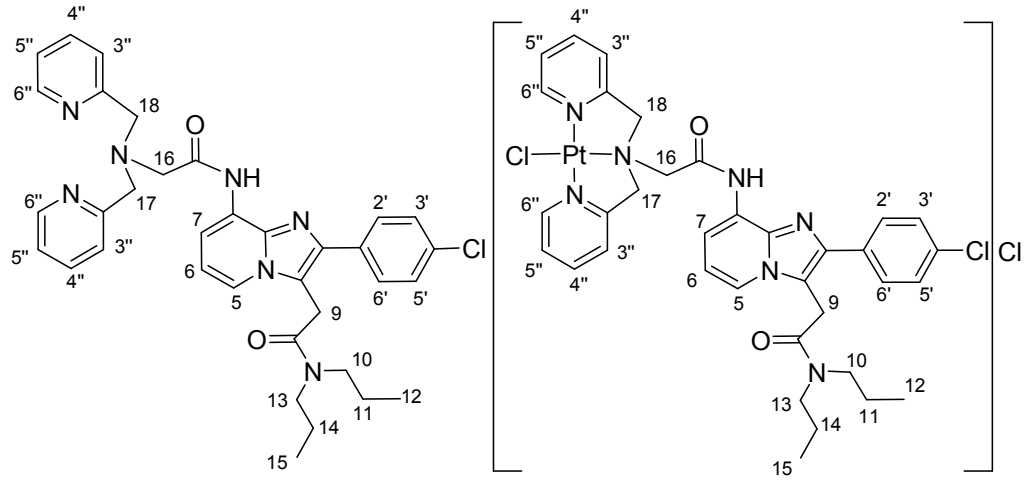

CB256 **1**

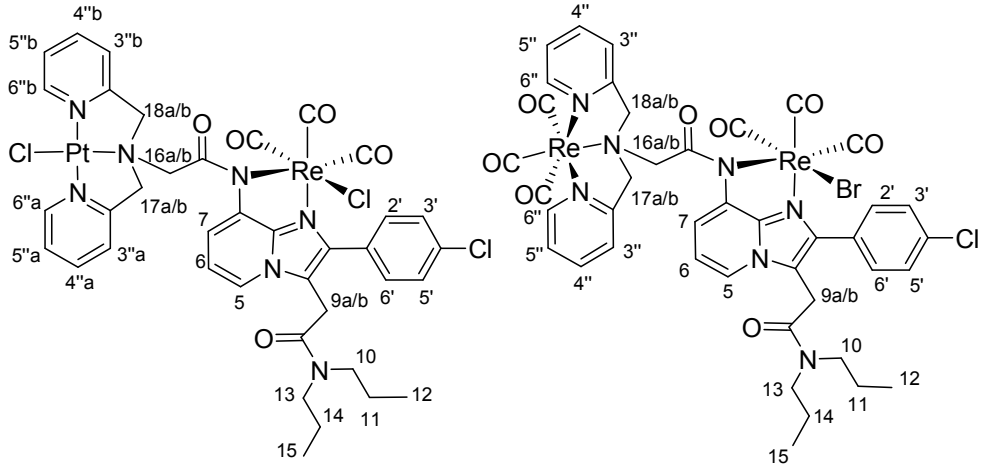

2 **3**

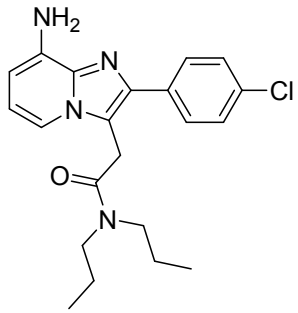

CB86

Chart 2: Sketches of the TSPO ligands **CB256** and **CB86**, and of the Pt and Re coordination compounds **1**, **2**, and **3** prepared in this work.

As starting complex for Re coordination we used *fac*-[$ReBr(CO)_3(OH_2)_2$] that, in solution, generates the well known *fac*-$[Re(CO)_3(OH_2)_3]^+$ aqua species. First discovered in 1994,[29] *fac*-$[Re(CO)_3(OH_2)_3]^+$ has proven to be an ideal cold model for searching the most suitable synthetic procedures to prepare ^{99m}Tc as well as $^{188/186}$Re radiopharmaceutical agents.[23,24,30-36]

For all synthesized compounds, *in vitro* studies have been performed to assess their affinity toward TSPO and their cytotoxic activity. In addition, platinum and rhenium cellular uptake (by ICP-MS), morphological analysis of the mitochondrion and of the nucleus (by fluorescence microscopy), as well as the ability of the newly synthesized compounds to cause collapse of the mitochondrial membrane potential ($\Delta\Psi_m$) and to interfere with the cell cycle progression of C6 glioma cells, have been investigated.

Experimental Section

Chemical methods. Commercial reagent grade chemicals, including [$ReBr(CO)_5$] and PK11195, and solvents were purchased from Sigma-Aldrich (Milan, Italy) and used without further purification. The radioligand [^{3}H]-PK11195 (85.7 Ci/mmol) was purchased from PerkinElmer Life Sciences. [2-(4-Chlorophenyl)-8-amino-imidazo[1,2-*a*]-pyridin-3-yl]-*N*,*N*-di-*n*-propylacetamide (CB86)[8] and 2-(8-(2-(bis(pyridin-2-yl-methyl)amino)acetamido)-2-(4-chlorophenyl)imidazo[1,2-a]pyridin-3-yl)-N,N-dipropylacetamide (CB256)[20] were prepared as already reported. ^{1}H NMR data for CB256 are reported in Table 1. ^{13}C-NMR of CB256 (DMSO-d_6): 148.5 (C6"), 136.3 (C4"), 129.2 (C2'/6'), 128.6 (C3'/5'), 122.8 (C3"), 122.1 (C5"), 119.4 (C5), 111.9 (C6), 108.8 (C7), 59.8 (C17/18), 58.5 (C16), 48.5 (C10), 46.8 (C13), 28.6 (C9), 21.4 (C11), 20.1 (C14), 10.9 (C12/15) ppm. $K[PtCl_3(\eta^2-C_2H_4)]$ (Zeise's salt) was prepared from

potassium tetrachloroplatinate and ethylene gas as already reported.[37] *fac*-[$ReBr(CO)_3(OH_2)_2$] was prepared from [$ReBr(CO)_5$] in water as already reported.[18,19]

Instrumental measurements. Electrospray ionisation mass spectrometry (ESI-MS) was performed with an electrospray interface and an ion trap mass spectrometer (1100 Series LC/MSD Trap system Agilent, Palo Alto, CA). FT-IR spectra were collected on a Perkin-Elmer IR Fourier transform spectrophotometer in KBr pellets. ^{1}H 1D and 2D COSY, NOESY, [^{1}H-^{13}C]-HSQC, and [^{1}H-^{15}N]-HSQC (natural abundance ^{15}N) spectra were recorded on Bruker Avance DPX 300 MHz and Avance II 600 MHz instruments. Standard Bruker pulse sequences were used for the NMR experiments using gradient selected versions when necessary. Chemical shifts are given in ppm. ^{1}H chemical shifts were referenced by using the residual protic peak of the solvent as internal reference (3.31 ppm for Methanol-d_4, 2.50 ppm for Dimethyl Sulfoxide-d_6, 2.05 ppm for Acetone-d_6, 4.80 ppm for Deuterium Oxide). ^{13}C chemical shifts were referenced by using the residual peak of the solvent as internal reference (39.51 ppm for Dimethyl Sulfoxide-d_6, 29.92 ppm for Acetone-d_6). ^{15}N chemical shifts were referenced to external $^{15}NH_4Cl$ (1M in 1M HCl) placed at 24 ppm.[38] ^{195}Pt chemical shifts were referenced to external K_2PtCl_4 (1M in 1M HCl) placed at −1620 ppm with respect to Na_2PtCl_6. Elemental analyses were carried out with an Eurovector EA 3000 CHN. ICP-MS determinations (Pt and Re) were performed using a Varian 820-MS instrument (Varian Inc., Lake Forest, CA, USA) equipped with a SPS 3 auto-sampler. The mass spectrometer was used in peak hopping mode. ICP was operated under hot plasma conditions for all elements. The optimized operating conditions were the following: Rf-power: 1400 W; nebulizer type: micro-concentric PFA 100 μL/min; nebulizer flow: 1.0 L/min; plasma gas flow rate: 18 L/min; auxiliary gas flow rate: 1.80 L/min; sampler and skimmer cone: Ni; quadrupole scan mode: peak hopping; detector: ETP.

Synthesis of [PtCl(CB256-*N,N,N*)]Cl (1). A solution of CB256 (25.6 mg, 0.041 mmol) in 5 mL of methanol was treated with Zeise's salt ($K[PtCl_3(\eta^2-C_2H_4)]$,16.0 mg, 0.041 mmol) and kept under stirring at 40 °C for 3 h meanwhile a white precipitate (KCl) formed. The suspension was cooled to room temperature and dried over Na_2SO_4. The mother liquor was filtered, concentrated under reduced pressure to a volume of *ca.* 2 mL, and treated with diethyl ether which caused the precipitation of the desired product as a white powder. The precipitate was left standing at 4 °C for 2 h and then was isolated by filtration of the mother solution, washed with diethyl ether, and dried under vacuum. The obtained solid was further washed with a small amount (100 μL) of water and dried under vacuum. Obtained 29.0 mg (70.5% yield). *Anal. Calculated* for [PtCl(CB256-*N,N,N*)]Cl·$3H_2O$ ($C_{35}H_{44}Cl_3N_7O_5Pt$): C, 44.52; H, 4.70; N, 10.38%. *Found*: C, 44.53; H, 4.49; N, 10.22%. *ESI-MS: calculated* for $[PtCl(CB256\text{-}N,N,N)]^+$ ($C_{35}H_{38}Cl_2N_7O_2Pt$) = 854.7. *Found*: *m/z* (% relative to the base peak) = 854.1 (100) $[M]^+$. ^{1}H-NMR data are reported in Table 1. ^{195}Pt-NMR (DMSO-d_6): -2324.2 ppm. ^{13}C-NMR (DMSO-d_6): 148.5 (C6"), 140.9 (C4"), 129.3 (C2'/6'), 128.4 (C3'/5'), 125.1 (C5"), 123.9 (C3"), 120.7 (C5), 112.4 (C7), 111.5 (C6), 67.0 (C17/18), 60.7 (C16), 48.7 (C10), 46.7 (C13), 28.7 (C9), 21.4 (C11), 20.3 (C14), 10.9 (C15), 10.7 (C12) ppm.

Synthesis of [{PtCl}(CB256-H$_{-1}$){ReCl(CO)$_3$}] (2). CB256 (70.0 mg, 0.11 mmol) was dissolved in 20 mL of CH_3OH and treated with Zeise's salt ($K[PtCl_3(\eta^2-C_2H_4)]$, 43.6 mg, 0.11 mmol). The resulting solution was kept under stirring at 40 °C for 4 h meanwhile a white precipitate (KCl) formed. The mother liquor was cooled to room temperature and dried over Na_2SO_4. After filtration, the solution was concentrated under reduced pressure to a volume of *ca.* 10 mL and treated with an excess of LiCl (191.0 mg, 4.5 mmol). After stirring at 40 °C for 10 min, the reaction mixture was treated with *fac*-$[ReBr(CO)_3(OH_2)_2]$ (87.1 mg,

0.22 mmol). Soon a white solid precipitated from solution. The reaction mixture was left under stirring for 3 h at 40 °C then filtered and the isolated white solid washed with a small amount of cold methanol and dried under vacuum. Obtained 53.0 mg (41.5% yield). *Anal. Calculated* for [{PtCl}(CB256-H$_{-1}$){ReCl(CO)$_3$}]·H$_2$O ($C_{38}H_{37}Cl_3N_7O_5PtRe$): C, 38.76; H, 3.34; N, 8.33%. *Found*: C, 38.79; H, 3.27; N, 8.42%. *ESI-MS: calculated* for [{PtCl}(CB256-H$_{-1}$){Re(CO)$_3$}]$^+$ ($C_{38}H_{37}Cl_2N_7O_5PtRe$) = 1123.1. *Found*: *m/z* (% relative to the base peak) = 1123.8 (100) [M – Cl]$^+$. A detailed description of the ^{1}H NMR spectra is given in the Electronic Supplementary Information (Figures S1 and S2 and Table 1). ^{13}C-NMR (Acetone-d$_6$): 149.8 (C6"a/b), 141.6 (C4"b), 141.3 (C4"a), 133.4 (C5"a), 129.2 (C3'/5'), 126.0 (C2'/6'), 125.8 (C5"b), 125.4 (C3"b), 125.1 (C3"a), 117.8 (C5), 117.3 (C7), 116.1 (C6), 67.9 (C17/18), 64.8 (C16), 50.1 (C10), 48.1 (C13), 29.5 (C9), 22.8 (C11), 21.5 (C14), 11.3 (C12/15) ppm.

Synthesis of [{Re(CO)$_3$}(CB256-H$_{-1}$){ReBr(CO)$_3$}] (3). CB256 (44.3 mg, 0.07 mmol) was dissolved in 3 mL of methanol and treated with 625 µL of a 0.13 M solution of KOH in methanol (0.08 mmol). After stirring for 15 min, *fac*-[ReBr(CO)$_3$(OH$_2$)$_2$] (60.4 mg, 0.15 mmol) was added to the methanolic solution and the reaction mixture was kept under stirring at 50 °C for 3 h and then at 35 °C for 15 h, meanwhile the desired product precipitated as a pale orange solid. The solid was isolated by filtration of the mother liquor, washed with diethyl ether, dried under vacuum, then washed with a small amount of cold water (100 µL) and dried again. Obtained 33.0 mg (38 % yield). *Anal. Calculated* for [{Re(CO)$_3$}(CB256-H$_{-1}$){Re(CO)$_3$Br}]·3.5H$_2$O ($C_{41}H_{44}BrClN_7O_{11.5}Re_2$): C, 37.65; H, 3.36; N, 7.50%. *Found*: C, 37.48; H, 3.00; N, 7.38%. *ESI-MS: calculated* for [{Re(CO)$_3$}(CB256-H$_{-1}$){Re(CO)$_3$}]$^+$ ($C_{41}H_{37}ClN_7O_8Re_2$) = 1163.6. *Found*: *m/z* (% relative

to the base peak) = 1163.7 (100) $[M - Br]^+$. A detailed description of the ^1H NMR spectra is given in the Electronic Supplementary Information (Figures S3 and S4 and Table 1). ^{13}C-NMR (Acetone-d_6): 152.5 (C6"a/b), 140.9 (C4"a/b), 133.6 (C2'/6'), 129.2 (C3'/5'), 126.3 (C5"a/b), 124.5 (C3"a/b), 117.8 (C7), 117.5 (C5), 116.3 (C6), 77.8 (C16), 69.3 (C18), 69.1 (C17), 50.2 (C13), 29.7 (C9), 48.2 (C10), 22.8 (C11), 21.6 (C14), 11.5 (C12/15) ppm.

Biological methods. DMEM nutrient, PBS, trypsin-EDTA, penicillin (10,000 U/mL), streptomycin (10 mg/mL), L-glutamine solution (100×), and fetal bovine serum (FBS) were purchased from Euroclone (Italy). Disposable culture flasks and Petri dishes were from Corning, Glassworks (Corning, N.Y., USA). Rat C6 glioma cells, from Interlab Cell Line Collection (ICLC) (Genova, Italy), and the cisplatin sensitive A2780 and the cisplatin resistant A2780cisR human ovarian carcinoma cell lines (kindly provided by Prof. Mauro Coluccia, University of Bari, Italy) were cultured in DMEM nutrient supplemented with 10% heat inactivated FBS, 2 mM L-glutamine, 100 U/mLpenicillin, and 100 μg/mL streptomycin in a 5% CO_2 humidified atmosphere at 37 °C.

Membrane preparation. Membranes from the tumor cells were prepared as described by Denora et al.[20]

Radioligand binding assay at TSPO. Binding of [^{3}H]-PK11195 at TSPO was performed according to a procedure previously reported.[20]

Cytotoxicity Assays. Cytotoxicity assays were carried out against rat C6 glioma cells expressing high levels of TSPO, and for free CB256 and platinum-coordination compounds **1** and **2** also against cisplatin-sensitive A2780 and cisplatin-resistant A2780cisR human ovarian carcinoma cell lines.[20] All tested compounds were dissolved in DMSO prior to their dilution with cell

culture medium to the predetermined experimental concentrations (eight concentrations ranging from 0.05 to 100 μM). Cytotoxicity (IC_{50}) values for the tested compounds were determined using the 3-(4,5-dimethylthiazol-2-yl)-2,5-diphenyltetrazolium bromide (MTT) assay, as previously reported.[20] Briefly, the cells were seeded in 96 wells plate and incubated at 37 °C for short (24 h) and long (72 h) periods with the tested compounds. Then 10 μL of 5 mg/mL MTT were added to each well and the plates incubated for additional 4 h at 37 °C. Subsequently, cells were lysed by addition of 150 μL of 50% (v/v) DMSO and 50% (v/v) ethanol solution, and absorbance of each individual well was measured by microplate reader at 570 nm (Wallac Victor3, 1420 Multilabel Counter, Perkin-Elmer). The reported values are the average of triplicate determinations made on at least three separate experiments.

Cellular uptake of platinum and rhenium. The uptake of compounds **1**, **2**, and **3** and of cisplatin, and *fac*-$[ReBr(CO)_3(OH_2)_2]$ as ereference compounds by C6 glioma cells was also measured. Cells were seeded in 60 mm tissue culture dishes at a density of ~30000 cells/cm^2. After 1 day of incubation at 37 °C in a humidified atmosphere with 5% CO_2, the culture medium was replaced with 2 mL of medium containing the tested compounds at a concentration of 1 μM and cells further incubated for 4 or 24 h. In this case DMF was used to dissolve the compounds prior to their dilution to the predetermined experimental concentration with cell culture medium. The percentage of the organic solvent used to dissolve the test compound never exceeded 1% (v/v) of the total. At the end of the incubation period, the cell monolayer was washed twice with ice-cold PBS and then digested with 2 mL of HNO_3(67%)/H_2O_2(30%) (1:1, v/v) for 4 h at 60 °C. Platinum and rhenium were quantified using inductively coupled plasma mass spectrometry (ICP-MS). All the experiments were performed in triplicate.

Fluorescence Microscopy. Wide field fluorescence of cells was analyzed through an inverted Zeiss Axiovert 200 microscope (Zeiss, Milano, Italy) equipped with a 63x1.4 oil objective, as reported by Denora *et al*.[20] C6 glioma cells were incubated for 24 h alone and in the presence of cisplatin, CB256, **1**, **2** or **3** at concentrations of 10 μM. Mitochondrial morphology and nuclear morphology of control cells and of cells treated with tested compounds were imaged by staining for 15-30 min at 37 °C and in 5% CO_2 atmosphere with 25 nM MitoTracker Red CMXRos and 1 μg/mL DAPI (Molecular Probes) used as mitochondrial and nuclear markers, respectively. Excitation of MitoTracker Red and of DAPI, as well as the selection of the emission fluorescence, was accomplished with appropriate filters mounted on Lambda 10-2 filter wheel controller (Sutter Instruments, Novato, CA). Fluorescence images were captured by a Cool-SNAPHQCCD camera (Roper Scientific, Trenton, NJ) using the Metamorph software (Universal Imaging Corporation). In each experiment, times of acquisition and light exposure were kept the same in order to compare emitted signal intensities.

Flow cytometry analysis of mitochondrial transmembrane potential ($\Delta\Psi_m$). C6 glioma cells were seeded at a density of 250,000 cells/plate and treated with compounds **1**, **2**, or **3** for 24 h at concentrations corresponding to their IC_{50} (25, 20, and 25 μM, respectively). The mitochondrial membrane potential ($\Delta\Psi_m$) was determined by labeling floating and adherent trypsinized cells with the fluorescent probe JC-1 by using previously reported procedures.[20]

Cell Cycle Perturbations studies. C6 glioma cells were dispensed at a density of 250,000 cells/plate. Following overnight incubation, cells were treated with compounds **1**, **2**, or **3** for 24 and 72 h at concentrations corresponding to their IC_{50} (25, 20, 25 μM, and 3, 5, 19 μM, respectively). Cell cycle determinations were performed using a FACScan flow cytometer

(Becton Dickinson) as previously described, and data were interpreted using the CellQuest and the ModFit software provided by the manufacturer.[20]

Statistical Analysis. All data are presented as the mean ± SD. The statistical analysis was accomplished using one-way analysis of variance (ANOVA) followed by the Tukey post hoc tests (GraphPad Prism, version 4, for Windows, GraphPad Software, San Diego, CA). Differences were considered statistically significant at $p < 0.05$.

Results and discussion

Chemistry

The recently prepared TSPO ligand CB256[20] has been used as a carrier for receptor-mediated drug delivery after loading with two fundamental metal ions used in medicinal inorganic chemistry: platinum(II) (with potential chemotherapic effects) and rhenium(I) [with potential application in diagnosis (if substituted with ^{99m}Tc) or in therapy (if substituted with $^{186/188}$Re)].

Synthesis of [PtCl(CB256-*N,N,N*)]Cl (1). Complex **1** was obtained by reaction of CB256 with Zeise's salt ($K[PtCl_3(\eta^2\text{-}C_2H_4)]$), in methanol. Zeise's salt is endowed with a high reactivity due to the presence of the coordinated ethylene molecule which renders the chloride in *trans* position a good leaving group.[37] Moreover, since during the reaction, gaseous ethylene is released and KCl precipitates, the reaction is clean and straightforward. Complex **1** (Chart 2) was characterized by elemental analysis, ESI-MS, and ^{1}H, ^{13}C, and ^{195}Pt–NMR in DMSO–d_6. The ^{1}H-NMR spectrum of **1** in DMSO–d_6 **(Figure 1)** shows in the range 5.6–4.0 ppm the presence of three signals assignable to the methylenic protons 9, 16, and 17/18 (see Chart 2 for numbering of protons).

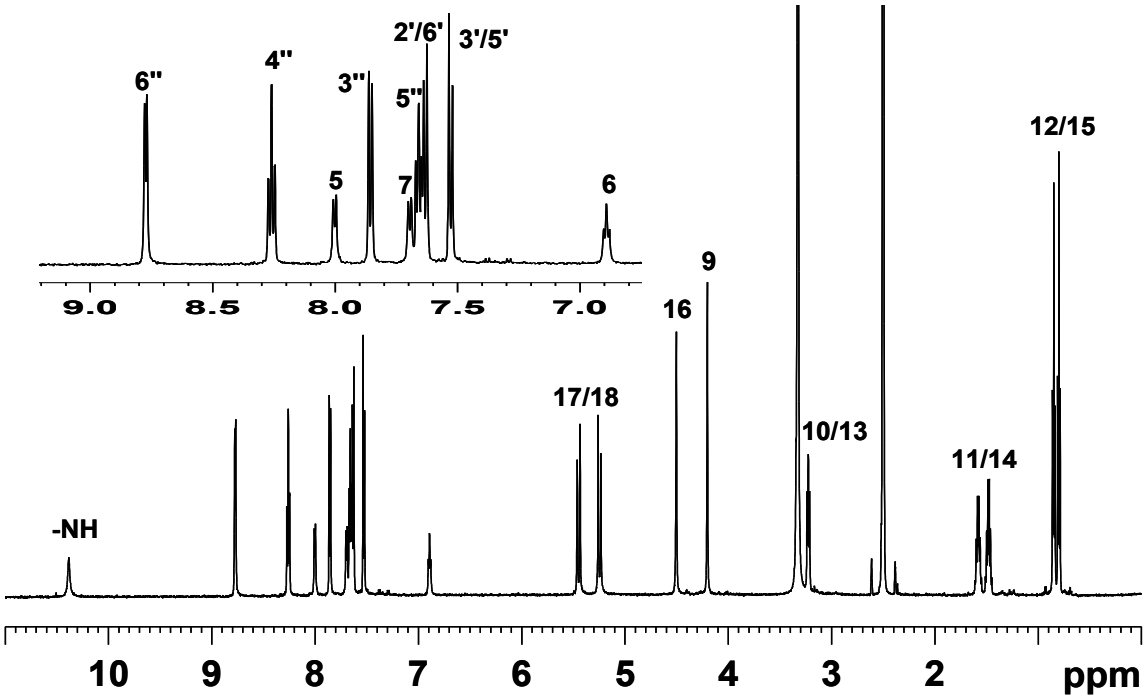

Figure 1: ^{1}H-NMR (600MHz) spectrum of **1** in DMSO–d_6.

The AB system falling at 5.34 ppm and integrating for 4 protons was assigned to the methylenic groups 17 and 18 (non-equivalent geminal protons). This signal is correlated by a NOESY cross peak to the doublet at 7.86 ppm (cross-peak A in Figure 2-A) assigned to protons 3" ($^{4}J_{H\text{-}H}$ = 7.80 Hz). The singlet falling at 4.50 ppm was assigned to the methylenic group 16 on the basis of the spatial correlations with the signals at 5.34 (cross-peak B in Figure 2-A) and 10.38 ppm (cross-peak C in Figure 2-A), this latter belonging to the amidic proton. The signal falling at 4.20 ppm was assigned to the methylenic group 9. This latter signal shows NOESY cross-peaks with the doublet falling at 7.63 ppm (2H, $^{3}J_{H\text{-}H}$ = 8.15 Hz) and assigned to protons 2'/6' of the 4-Cl-phenyl group (D in Figure 2-A), and with the doublet falling at 8.00 ppm (1H, $^{3}J_{H\text{-}H}$ = 6.94 Hz) assigned to the proton in position 5 of the imidazopyridine ring system (E in Figure 2-A). Thus the doublet at 7.53 ppm (2H, $^{3}J_{H\text{-}H}$ = 8.15 Hz), which shows NOESY and COSY cross-peaks with the doublet at 7.63 ppm, was assigned to protons 3'/5' of the 4-Cl-phenyl group. The

characterization of the imidazopyridine ring system was completed by assigning the triplet at 6.89 ppm (1H, $^{3}J_{H\text{-}H}$ = 7.11 Hz) to proton 6 on the basis of NOESY (F and G in Figure 2-A) and COSY cross-peaks with the doublets falling at 8.00 (proton 5) and 7.69 ppm (1H, $^{3}J_{H\text{-}H}$ = 7.46 Hz; proton 7). The characterization of the dipicolylaminic residue started from the assignment of the doublet falling at 8.77 ppm (2H, $^{3}J_{H\text{-}H}$ = 5.55 Hz) to protons 6", which are the less shielded due to their closeness to the pyridinic nitrogen. The coordination to the metal core of the pyridinic nitrogens is confirmed by the deshielding of protons 6" with respect to the free ligand ($\Delta\delta$ = 0.30 ppm in DMSO–d_6; see also Table 1). The triplet at 7.66 ppm (2H, $^{3}J_{H\text{-}H}$ = 6.59 Hz) shows a COSY cross-peak (I in Figure 2-B) with the signal related to protons 6" and was assigned to protons 5". In addition, the signal at 7.66 ppm shows a COSY cross-peak (H in Figure 2-B) with the signal at 8.26 ppm which was assigned to protons 4".

The characterization of the dipropylacetamidic chains started from the triplet at 3.23 ppm which was assigned to methylene 13 due to the absence of a NOESY cross-peak with methylene 9 (also in free CB256 there was no correlation between methylenes 9 and 13). As a consequence, the multiplet falling at 1.48 ppm (2H, $^{3}J_{H\text{-}H}$ = 7.48 Hz) was assigned to methylene 14 and the triplet at 0.80 ppm (3H, $^{3}J_{H\text{-}H}$ = 7.26 Hz) to methyl 15. Methylene 10, belonging to the second propylacetamidic chain, overlaps with the solvent signal at 3.32 ppm and is correlated to the multiplet centred at 1.56 ppm, assigned to methylene 11, and to the triplet at 0.85 ppm, assigned to methyl 12.

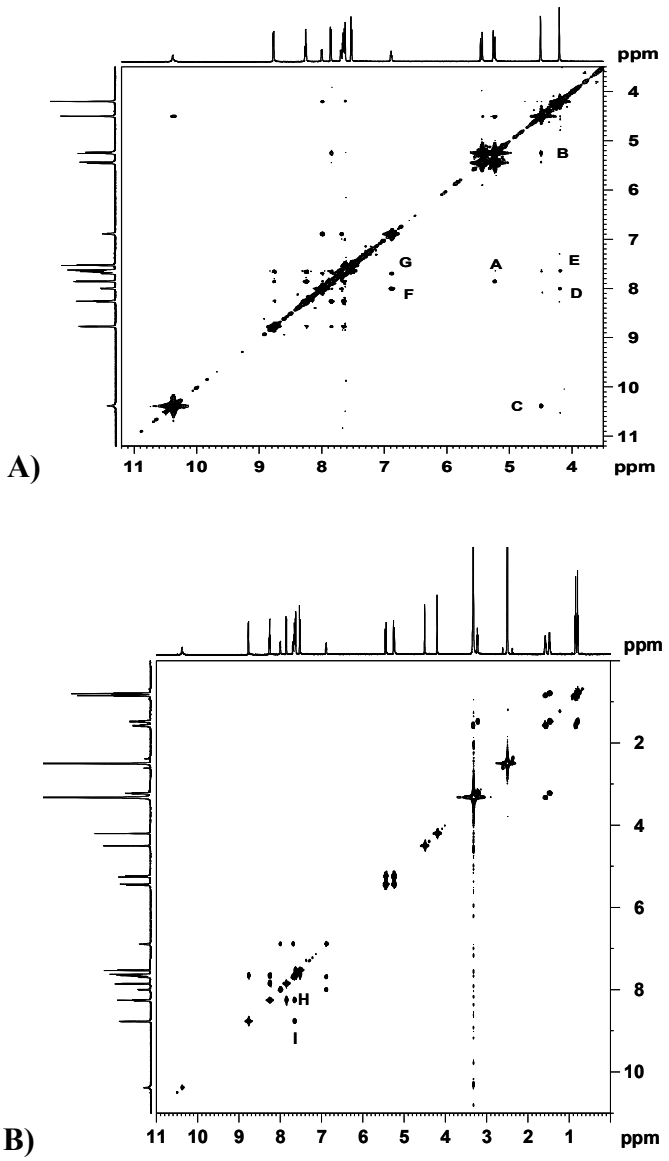

Figure 2: Portions of the 2D NOESY (**A**) and COSY (**B**) spectra (600MHz) of **1** in DMSO–d_6.

The ^{195}Pt–NMR spectrum of **1** in DMSO–d_6 showed one broad signal at –2324.2 ppm, a chemical shift compatible with a Pt atom in a N_3Cl coordination environment.

Synthesis of [{PtCl}(CB256-H$_{-1}$){ReCl(CO)$_3$}] (2). Complex **2** was synthesized following a two-steps, one-pot, procedure. In the first step, CB256 was reacted with Zeise's salt to form the

intermediate (not isolated) complex [PtCl(CB256-*N,N,N*)]Cl; in the second step, the intermediate platinum complex was reacted with rhenium tricarbonyl (in the presence of an excess of LiCl) to give the desired product as a white precipitate. The excess of LiCl favours the obtainment of the species having rhenium-coordinated chloride.

Complex **2** (Chart 2) was characterized by elemental analysis, ESI-MS, and ^{1}H- and ^{13}C-NMR as described in the Experimental Section and in the Electronic Supplementary Information. Here we want to notice that, because of the asymmetry of the rhenium center, the two protons of each methylenic group become diastereotopic and generate an AB spin system (see the Electronic Supplementary Information and Table 1).

Synthesis of [{Re(CO)$_3$}(CB256-H$_{-1}$){ReBr(CO)$_3$}] (3). Complex **3** was obtained by reaction of CB256 with two equivalents of *fac*-[ReBr(CO)$_3$(OH$_2$)$_2$], in methanol. The first rhenium residue coordinates to the dipicolylaminic portion, while the second rhenium atom coordinates to the imidazopyridine ring system with deprotonation of the amidic group in position 8 following treatment with a slight excess of KOH.

Also complex **3** (Chart 2) was characterized by elemental analysis, ESI-MS, and ^{1}H- and ^{13}C-NMR as detailed in the Experimental Section and in the Electronic Supplementary Information. Also for compound **3**, because of the asymmetry of the rhenium center bound to the imidazopyridine system, the two protons of each methylenic group become diastereotopic and generate an AB spin system in the ^{1}H NMR spectrum.

Biology

Radioligand Binding Assays. The affinity for TSPO of the metal complexes **1**, **2**, and **3** was evaluated by measuring their ability to displace the reference compound [^{3}H]-PK11195 from binding to the membrane of C6 glioma cells overexpressing TSPO.[39] The results, reported in **Table 2**, were compared to those obtained for CB256. This latter has an appreciable affinity for TSPO (239 nM),[20] which, however, is lower than that of the reference compound PK11195 (0.4 nM) and of its precursor CB86 (1.6 nM).[13] Probably, the reduced affinity for TSPO of CB256 stems from the steric bulk generated by the dipicolylaminic moiety at position 8 of the imidazopyridine nucleus, which is crucial for the interaction of the ligand with mitochondrial TSPO.[15] Among the metal complexes, only the Pt complex **1** showed an affinity (326 nM) comparable to that of the free ligand. In contrast, the dinuclear Re complex **3** and the heteronuclear Pt-Re complex **2** did not show appreciable affinity for the target receptor (1 μM concentration of **2** and **3** can displace, respectively, 35 and 40% of the reference compound [^{3}H]-PK11195 from the C6 glioma cell membrane (**Table 2**)). These results indicate that while metal-ion coordination to the tridentate bis-(2-pycolyl)amine residue does not significantly alter the TSPO affinity of CB256, in contrast, metallation at the imidazopyridine moiety greatly reduces the affinity for TSPO. Moreover, the reduced TSPO affinity of CB256, as compared to the precursor ligand CB86, suggests the need for a longer spacer between the imidazopyridine moiety and the tridentate metal-binding group.

Cytotoxicity Assays

Table 3 summarizes the cytotoxicity of CB256 and compounds **1**, **2**, and **3** against rat C6 glioma cells selected for their high level of TSPO expression and exposed for a period of 72 h. Cisplatin was used as reference compound. Our previous investigation has shown that CB256 is extremely effective (IC_{50} value of 0.3 to be compared with a value of 0.7 μM for cisplatin; Table 3). The

high cytotoxicity of CB256 was correlated to its ability to produce double-strand lesions on DNA after coordination of a biometal, such as Cu(I).[20]

Compounds **1** and **2** are characterized by quite lower cytotoxicity towards C6 glioma cells than cisplatin (IC_{50} values of 3.1 and 4.5 μM for **1** and **2**, respectively). The lower cytotoxicity of **1** and **2** with respect to uncoordinated CB256 can be explained with their inability to load a biometal (Cu^{I}) and act as a double-strand breaker of DNA.[20,22] Moreover, the lower activity of compounds **1** and **2** with respect to cisplatin can be explained with their characteristic of monofunctional platinum drugs (unlike cisplatin, only one position is available on Pt for coordination to DNA). However, the activity of **1** and **2** is higher than that found for analogous monofunctional compounds with simple amines such as $[PtCl(dien)]^{+}$.[40]

As expected, the only-rhenium complex **3** (IC_{50} values of 19 μM) is the less effective of the complexes here investigated.

The cytotoxic activities of cisplatin, CB256, **1**, and **2** were also determined against the cisplatin sensitive A2780 and the cisplatin resistant A2780cisR human ovarian carcinoma cell lines exposed for 72 h.[41] A2780cisR cells are resistant to cisplatin due to a combination of decreased uptake, enhanced DNA repair/tolerance, and enhanced GSH levels.[41] As shown in Table 3, CB256, **1**, and **2** are less effective than cisplatin toward A2780 cells and, on the average, equally effective against the A2780cisR cell line. Interestingly, CB256 and **1**, unlike cisplatin, are equally active toward the sensitive and the resistant cell lines as evidenced by their resistance factor, defined as IC_{50}(resistant)/IC_{50}(sensitive), which is close to 1.

The lower cytotoxicity of the platinum derivatives **1** and **2**, with respect to free CB256 confirms that the antitumour activity of CB256 stems from its ability to coordinate a biometal and act as a DNA-damaging agent.

Cellular Uptake.

To examine the drug cellular uptake, C6 glioma cells were exposed to compounds **1**, **2**, and **3** at a concentration of 1 μM for a short (4 h) and a long time (24 h), and the intracellular platinum or rhenium content was measured by inductively coupled plasma mass spectrometry. Cisplatin and *fac*-$[ReBr(CO)_3(OH_2)_2]$ were used as reference compounds, always at a concentration of 1 μM (Table 4). Interestingly, the uptake of compounds **1** and **2** was, respectively, 32- and 47-fold greater than that of cisplatin after just 4 h of incubation and remained considerably higher (about 16 and 28 times greater) also after 24 h. A similar trend was observed for rhenium uptake by glioma cells, the uptake of **2** and **3** was, respectively, 28 and 127-fold greater than that of *fac*-$[ReBr(CO)_3(OH_2)_2]$, after 4 h incubation, and remained considerably greater also after 24 h exposure time (14 and 63-fold greater for **2** and **3**, respectively). It should be noted that **3** carries two Re atoms, which can explain, at least in part, the greater uptake observed for **3** as compared to **2**. All complexes exhibit a cellular uptake much greater than that of the reference compounds cisplatin and *fac*-$[ReBr(CO)_3(OH_2)_2]$. This can be ascribed to an increased lipophilicity of the metal complexes leading to enhanced passive diffusion across the cellular membrane. The latter possibility is supported by the capacity factors (log k_0) of compounds **1**, **2**, and **3** measured by HPLC analysis (data not shown).

In conclusion, the results of the cellular uptake clearly indicate that conjugation with a TSPO ligand can greatly increase the cellular uptake of the metallo-drugs.

Mitochondrial and nuclear morphology modification

Cisplatin-DNA adducts are known to cause various cellular responses, such as replication arrest, transcription inhibition, cell-cycle arrest, and apoptosis.[42] Moreover, TSPO ligands act on mitochondria exerting a proapoptotic activity. Therefore, we analyzed the structure of these organelles and of the nuclei in cells treated with **1**, and **2** and compared the results with those obtained with cisplatin and CB256. MitoTracker Red and DAPI dyes were used as mitochondrial and nuclear specific markers, respectively. The C6 glioma cells were incubated with cisplatin or with compounds CB256, **1** and **2** at a concentration of 10 μM for 24 h, and the mitochondrial and nuclear structure modifications were evaluated using a digital imaging system. Figure 3 shows representative images of control C6 glioma cells where the typical nucleus and the tubular interconnected mitochondrial network are evident. In contrast, cells treated with cisplatin, CB256, **1**, and **2** exhibit marked morphological alteration of the organelles and of the nucleus after 24 h of incubation. In particular, cells exhibit fragmented nuclei and mitochondria with MitoTracker Red diffused in the cytosol. These data represent a clear evidence that the tested compounds induce cell death also by targeting mitochondria.

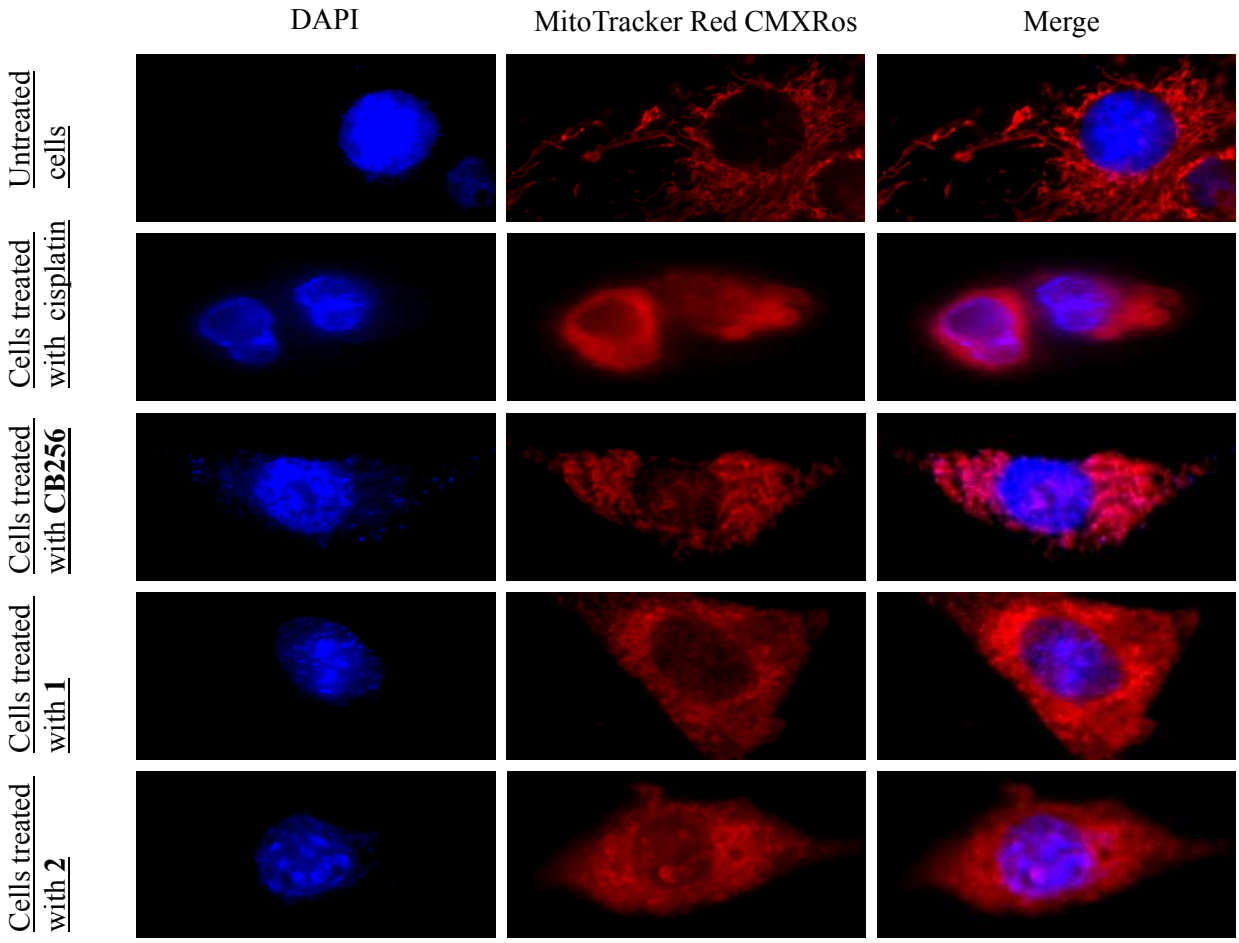

Figure 3. Morphological analysis of the mitochondrial network structure and of the nucleus in C6 glioma cells. Cells seeded onto 24 mm coverslips (~100,000 cells/well) were treated with 10 μM of CB256, **1**, **2**, or cisplatin at 37 °C in a 5% CO_2 atmosphere and incubated for 24 h. Mitochondrial and nuclear structures were evaluated by incubation of cells with 25 nM MitoTracker Red CMXRos and with 1 μg/mL DAPI, respectively. Mitochondria and nuclei of untreated cells are shown for reference. Images are representative of two independent experiments in which more than 10 cells were examined.

Flow cytometry analysis of mitochondrial transmembrane potential ($\Delta\Psi_m$)

The mitochondrial membrane potential ($\Delta\Psi_m$) was evaluated by using the mitochondria-specific fluorescent probe 5,5',6,6'-tetrachloro-1,1',3,3'-tetraethylbenzimidazolcarbocyanine iodide, also named JC-1. Cytofluorimetric analysis of JC-1-loaded C6 cells showed that only a small

percentage of control cells had depolarized mitochondria (0.2 %). On the contrary, as shown in Figure 4, an increased number of cells with depolarized mitochondria was observed in C6 cells exposed to compounds CB256, **1**, **2**, **3**, or cisplatin for 24 h (2.5, 3.4, 1.1, 0.7, and 18.2 %, respectively; Table 5). In particular, CB256, **1**, and **2** are effective, and induce $\Delta\Psi_m$ dissipation, an event that is known to precede the cell death by apoptosis. These data are in good agreement with the morphological analysis evidenced by fluorescence microscopy. As expected, the rhenium complex **3** was less effective than the platinum complexes **1** and **2** and only a small percentage of cells had depolarized mitochondria (0.7 %).

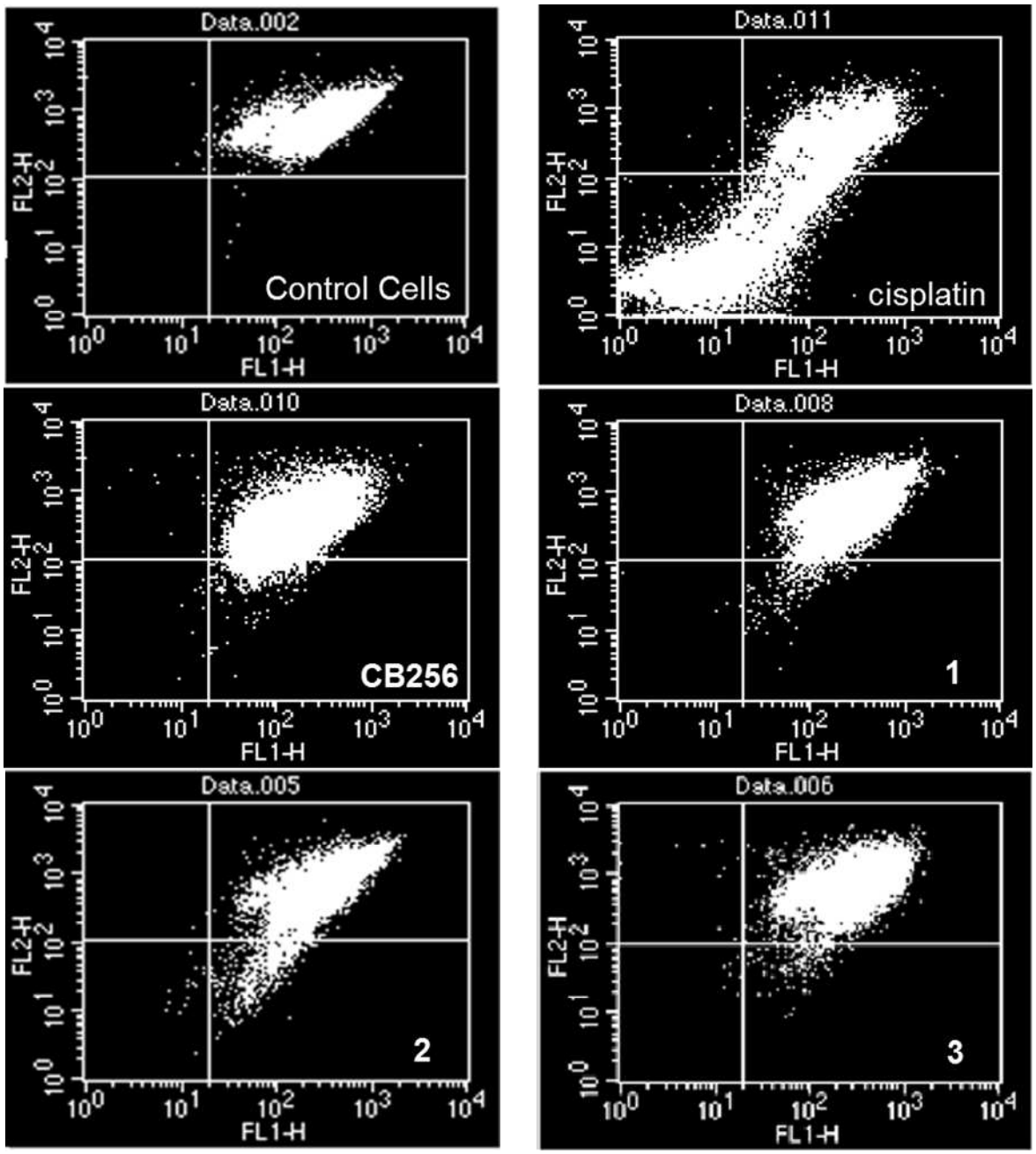

Figure 4. Effect of $\Delta\Psi_m$ dissipation on C6 glioma cells exposed to CB256[a], **1**, **2**, **3**, or cisplatin[a] for 24 h. Untreated cells were used as control. [a]From reference 20.

Cell Cycle Perturbation studies

To highlight the antiproliferative activity of **1**, **2**, and **3**, their ability to interfere with the C6 glioma cell cycle progression was evaluated by flow cytometry and the results compared to those obtained with free CB256 and cisplatin. Cells were exposed to **1**, **2**, **3**, or cisplatin (25, 20, 25, and 10 μM, respectively) for 24 h. As shown in Figure 5, only cisplatin showed a marked accumulation of cells in the G2/M phase suggesting an arrest of the cell cycle. Unlike cisplatin, cells treated with CB256, **1**, **2**, and **3** showed quite normal cell cycle histograms suggesting that, after 24 h of incubation, the residual cells begin to cycle (Figure 5). Moreover, cells were incubated for 72 h with the same compounds (CB256, **1**, **2**, **3**, or cisplatin) in concentrations corresponding to their IC_{50}, (i.e. 0.3, 3, 5, 19, and 5 μM, respectively). After 72 h of incubation, sub-G1 hypoploid cell population, indicating apoptosis, was observed in the cells treated with CB256, **1**, and **2**, as compared to the control (Table 6). This result is in accord with that observed by K. Datta *et al*.[43] for glioma cells sensitized to cisplatin by abrogating the p53 response with antisense oligonucleotides. As expected, the dirhenium complex **3** showed a sub-G1 hypoploid cell population similar to that measured for control cells.

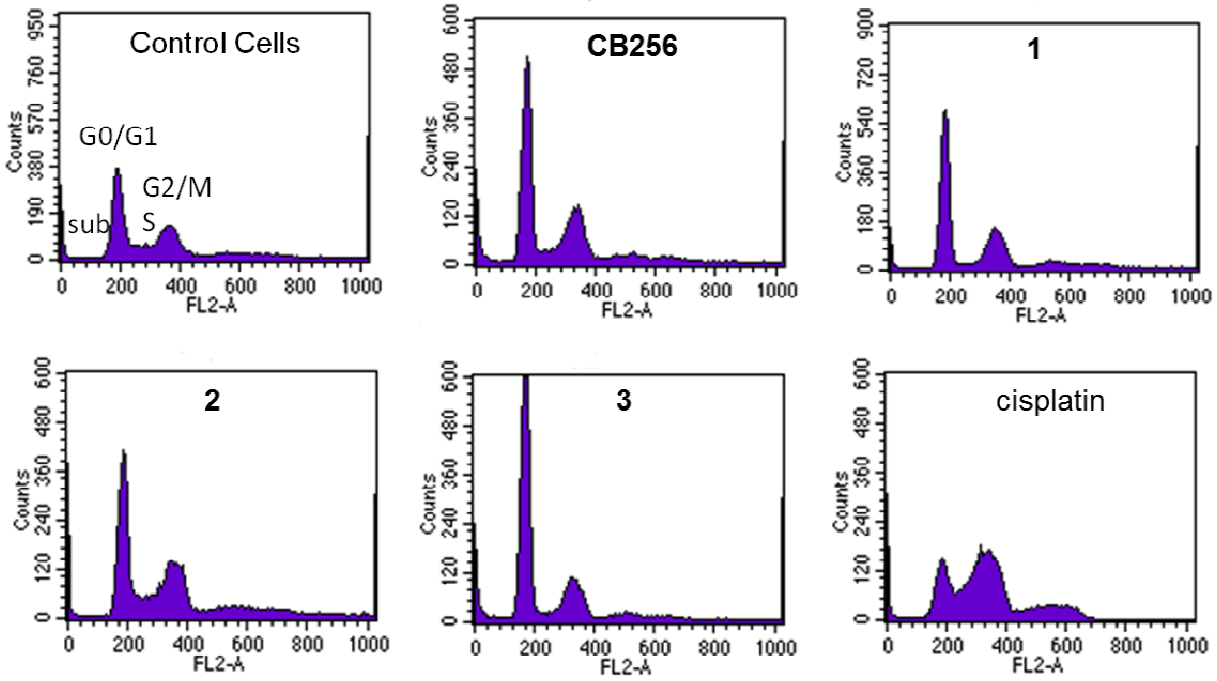

Figure 5. Flow cytometric analysis of C6 glioma cells following exposure to CB256 (from reference 20), **1**, **2**, **3**, or cisplatin (10, 25, 20, 25, and 10 μM, respectively) for 24 h. Untreated cells were used as control.

Conclusion

In this work, the 2-phenyl-imidazopyridin-dipropylacetamide TSPO ligand CB256 was loaded with platinum and/or rhenium to obtain a diagnostic or a therapeutic drug (this impies substitution of cold rhenium with either γ emitting ^{99m}Tc or β^- emitting $^{186/188}$Re). The presence of two metal-binding sites suggested also the possibility of simultaneous binding of a diagnostic and a therapeutic agent so affording a theranostic drug. So far we have prepared one mononuclear Pt(II) (**1**) and two dinuclear Pt(II)-Re(I) (**2**) and Re(I)-Re(I) (**3**) complexes. To the best of our knowledge, compound **2** is the first bimetallic Re/Pt-complex with potential theranostic applications reported so far. As aimed to, the new compounds exhibit a markedly

increased cellular uptake with respect to the reference compounds cisplatin and *fac*-$[ReBr(CO)_3(H_2O)_2]$. Such an increased cellular uptake depends, at least in part, upon an increased lipophilicity favoring diffusion across the cellular membrane. Facilitated transport through the cell membrane by OCT carriers might also play a role.

The free TSPO ligand CB256 proved to be the most active of all compounds and it was shown that its loading with a biometal (such as Cu^I) can induce double-strand breaks in DNA. Such a possibility is prevented if the dipicolylamine moiety is engaged in coordination to Pt^{II} or Re^I. To investigate the mechanism of the antiproliferative activity, we evaluated the ability of complexes **1**, **2**, and **3** to cause collapse of the mitochondrial membrane potential ($\Delta\Psi_m$) and to interfere with the cell-cycle progression of glioma C6 cells. These data, together with the mitochondrial and nuclear morphology modifications evidenced by fluorescence microscopy, suggest that **1** and **2**, like CB256 and cisplatin, are able to induce apoptosis in cancer cells. Unfortunately, coordination of Re to the imidazopyridine residue of CB256 strongly reduces its affinity towards TSPO. Therefore we are presently exploring the possibility to place the coordinating moiety (the dipicolylamine in the present case) in a different position of the imidazopyridine moiety so to improve the affinity for TSPO and possibly also inhibit the coordination of a metal ion to the same imidazopyridine moiety.

Electronic Supporting Information. NMR characterization (1D ^1H and 2D NOESY and COSY spectra) of complexes **2** and **3**.

Acknowledgments

The University of Bari (Italy), the Italian Ministero dell'Università e della Ricerca (MIUR; FIRB RINAME RBAP114AMK, PON02_00607_3621894, NANO Molecular tEcnologies for Drug delivery-NANOMED, PRIN 2010-2011), the European Union (COST CM1105, Metallo-Drug Design and Action), and the Inter-University Consortium for Research on the Chemistry of Metal Ions in Biological Systems (C.I.R.C.M.S.B.) are gratefully acknowledged.

Table 1. ^{1}H NMR Chemical Shifts (ppm) for **CB256**[a] and compounds **1**, **2**, and **3** in different solvents. $J_{H\text{-}H}$ (Hz) are reported in parentheses.*

	cmpd							
	CB256 (DMSO-d_6)	**CB256** (MeOH-d_4)	**CB256** (Acetone-d_6)	**1** (DMSO-d_6)	**1** (MeOH-d_4)	**1** (D_2O)	**2** (Acetone-d_6)	**3** (Acetone-d_6)
5	7.95 d (6.24)	7.92 d (7.24)	7.96 br	8.00 d (6.94)	7.98 d (6.70)	7.91 d (6.99)	7.82 d (6.60)	7.86 d (6.60)
6	6.89 t (7.35)	6.87 t (7.40)	6.84 t (7.16)	6.89 t (7.11)	6.89 t (7.18)	6.86 t (7.20)	6.93 t (7.33)	6.94 t (7.11)
7	7.96 d (7.02)	7.96 d (7.50)	8.07 d (7.76)	7.69 d (7.46)	7.81 d (7.48)	7.27 d (7.34)	8.39 d (7.70)	8.54 d (7.70)
9	4.26 s	4.29 s	4.32 s	4.20 s	4.23 s	4.10 s	4.13 pq (16.78)	4.14 pq (17.07)
10/13	3.37/3.24 t (7.66/7.66)	3.39/3.35 t (7.90/7.90)	3.46/3.33 t (7.73/7.50)	3.32/3.23 t (n.d./7.48)	3.38/n.d. t (7.62/n.d.)	3.34/3.29 t (7.12/7.12)	3.40–3.10 m (7.46/7.46)	3.40–3.15 br
11/14	1.61/1.50 m (7.50/7.50)	1.68/1.61 m (7.90/7.90)	1.69/1.57 m (7.96/7.96)	1.56/1.48 m (7.48/7.48)	1.66/1.59 m (7.62/7.62)	1.66/1.59 m (7.47/7.47)	1.70–1.40 m (7.79/7.79)	1.70–1.40 m (7.67/7.67)
12/15	0.87/0.81 t (7.37/7.30)	0.92/0.90 t (7.62/7.60)	0.90/0.85 t (7.26/7.26)	0.85/0.80 t (7.37/7.26)	0.91/0.89 t (7.20/7.20)	0.83/0.80 t (7.47/7.47)	0.90–0.70 m (7.26/7.36)	0.90–0.75 m (7.37/7.25)
16a/b	3.52 s	3.57 s	3.52 s	4.50 s	4.27 s	4.19 s	5.19/4.46 d (16.09/16.04)	5.82/5.05 d (15.36/15.65)
17a/b	3.94 s	4.02 s	3.98 s	5.34 pq (16.06)	5.34 s	5.20 pq (16.05)	5.96/5.31 d (16.19/16.27)	5.48/4.96 d (17.20/17.07)
18a/b							5.49/5.19 d (16.03/17.00)	5.87/5.13 d (17.21/17.64)
3''a/b	7.81 d (7.80)	7.90 d (6.00)	7.47 br	7.86 d (7.80)	7.74 d (8.10)	7.63 d (7.69)	7.91/7.71 d (8.01/7.84)	7.74 t (7.73)
4''a/b	7.54 t (8.66)	7.58–7.54 t (7.97)	7.53 m (7.63)	8.26 t (7.46)	8.18 t (7.95)	8.08 t (7.70)	8.27/8.16 t (8.01/7.84)	8.03 m (7.40)
5''a/b	7.21 m (6.83)	7.22 m (6.62)	7.17 m (6.82)	7.66 t (6.59)	7.58 t (6.79)	7.46 t (6.64)	7.68/7.63 t (6.59/6.77)	7.50–7.40 br
6''a/b	8.47 d (4.00)	8.43 d (4.56)	8.49 d (4.74)	8.77 d (5.55)	8.89 d (5.30)	8.69 d (5.59)	8.95/8.90 d (5.49/5.74)	8.97 br
2'/6'	7.76 d (8.26)	7.77 d (8.55)	7.89 d (8.55)	7.63 d (8.15)	7.60 d (8.26)	7.50 s	7.78 d (8.43)	7.90 d (8.07)
3'/5'	7.61 d (8.26)	7.55 d (8.54)	7.57 d (8.55)	7.53 d (8.15)	7.48 d (8.26)		7.48 d (8.43)	7.54 d (8.07)
NH	10.65 br	n.d.	10.78 br	10.38 br	n.d	n.d	-	-

*Numbering is as reported in **Chart 2**. s = singlet, d = doublet, t = triplet, pq = pseudoquartet, m = multiplet, br = broad, n.d. = not detected. [a]From reference 20.

Table 2. Affinities (K_i, nM) for TSPO on membrane extracts of C6 glioma cells.

Compound	K_i (nM)
PK11195	0.4 ± 0.05
CB256[a]	239 ± 43
1	326 ± 20
2	> 1000 (35%)[c]
3	> 1000 (40%)[c]
CB86[b]	1.6

[a]From reference 20. [b]From reference 13. [c]In parenthesis the percentage of [^{3}H]-PK11195 displaced at a concentration of the tested compound of 1 μM.

Table 3. Cytotoxicity of CB256, **1**, **2**, **3**, and cisplatin toward C6, A2780, and A2780cisR cancer cell lines.

Compound	**IC_{50} (μM)**		
	C6[a]	**A2780**[b]	**A2780cisR**[b,c]
CB256[d]	0.3 ± 0.1	9.0 ± 0.4	9.2 ± 0.4 (1.0)
1	3.1 ± 0.1	10.3 ± 0.4	10.4 ± 0.3 (1.0)
2	4.5 ± 0.1	10.6 ± 0.3	19.1 ± 0.6 (1.8)
3	19.2 ± 0.6	-	-
cisplatin[d]	0.7 ± 0.2	2.9 ± 0.4	9.2 ± 0.4 (3.1)

[a]Cells were seeded at a density of ~5000 cells/well into 96-well microtiter plates. Following overnight incubation, cells were treated with a range of drug concentrations (from 0.05 to 100 μM) and incubated at 37 °C in a humidified atmosphere with 5% CO_2 for a period of 72 h. Data are the mean values ± SD of three independent experiments performed in duplicate.[b]Cells were seeded in 96-wellplates at a density of ~10000 cells/well and incubated at 37 °C in a humidified atmosphere with 5% CO_2 for a period of 72 h in the presence of different concentrations of the tested compounds (from 0.05 to 100 μM). Data are the mean values ± SD of three independent experiments performed in duplicate. [c]Resistance factor, defined as IC_{50}(resistant)/IC_{50}(sensitive), is given in parentheses. [d]From reference 20.

Table 4. Uptake by C6 glioma cells of cisplatin, *fac*-[$ReBr(CO)_3(OH_2)_2$], and compounds **1**, **2**, and **3**.

	Platinum uptake by C6 glioma cells (ppb)[a]			**Rhenium uptake by C6 glioma cells (ppb)[a]**		
	cisplatin	**1**	**2**	*fac*-[$ReBr(CO)_3(OH_2)_2$]	**2**	**3**
after 4 h treatment	0.06 ± 0.01	1.9 ± 0.2	2.8 ± 0.1	0.08 ± 0.01	2.4 ± 0.2	10.5 ± 1.5
after 24 h treatment	0.14 ± 0.01	2.3 ± 0.3	3.9 ± 0.3	0.22 ± 0.02	3.2 ± 0.2	13.9 ± 0.9

[a]Cells were seeded in 60 mm tissue culture dishes at a density of ~30000 cells/cm^2 and exposed at a drug concentration of 1 μM for a short (4 h) and a long (24 h) time.

Table 5. Percentages of dead or suffering cells after 24 h incubation with compounds CB256, **1**, **2**, **3**, or cisplatin.

	% of dead or suffering cells[a]
Control cells	0.2 ± 0.1
CB256[b]	2.5 ± 0.1
1	3.4 ± 0.1
2	1.1 ± 0.1
3	0.7 ± 0.1
cisplatin	18.2 ± 0.7

[a]Cells seeded at a density of 250,000 cells/plate were treated with CB256, **1**, **2**, **3**, or cisplatin (10, 25, 20, 25, 10 μM, respectively) and incubated for 24 h. Untreated cells were used as control. The mitochondrial membrane potential ($\Delta\Psi_m$) was determined by labeling floating and adherent trypsinized control and treated cells with the fluorescent probe JC-1. The experiment was performed in duplicate. [b]From reference 20.

Table 6. Percentages of C6 glioma cells in sub-G1, G0/G1, S, and G2/M cell cycle phase after treatment with compounds CB256, **1**, **2**, and **3** for 72 h.

	% of cells in cell cycle phases[a]			
	sub-G1	**G0/G1**	**S**	**G2/M**
Control cells	5.9 ± 0.2	54.9 ± 2.2	11.1 ± 0.4	28.0 ± 1.1
CB256[b]	9.1 ± 0.4	49.1 ± 2.0	13.2 ± 0.5	28.7 ± 1.1
1	12.1 ± 0.5	53.2 ± 2.1	11.5 ± 0.5	23.1 ± 0.9
2	6.5 ± 0.3	55.6 ± 2.3	10.5 ± 0.4	27.4 ± 1.1
3	5.5 ± 0.2	54.4 ± 2.8	10.8 ± 0.4	29.4 ± 1.2

[a]Cells seeded at a density of 250,000 cells/plate were treated with compounds CB256, **1**, **2**, or **3** (0.3, 3, 5, 19, 5 μM, respectively) and incubated for 72 h. Untreated cells were used as control. The experiment was performed in duplicate. [b]From reference 20.

References

(1) V. Papadopoulos, M. Baraldi, T. R. Guilarte, T. B. Knudsen, J.-J. Lacapère, P. Lindemann, M. D. Norenberg, D. Nutt, A. Weizman, M.-R. Zhang, M. Gavish, *Trends Pharmacol. Sci.,* 2006, **27**, 402-409.

(2) R. Rupprecht, V. Papadopoulos, G. Rammes, T.C. Baghai, J. Fan, N. Akula, G. Groyer, D. Adams, M. Schumacher, *Nature Review/Drug Discovery,* 2010*,* **9**, 971-988.

(3) G. Trapani, N. Denora, A. Trapani, V. Laquintana, *J. Drug Target*., 2012, **20**, 1-22.

(4) N. Denora, T. Cassano, V. Laquintana, A. Lopalco, A. Trapani, C.S. Cimmino, L. Laconca, A. Giuffrida, G. Trapani, *Int. J. Pharm*., 2012, **437**, 221-231.

(5) S. Galiegue, N. Tinel, P. Casellas, *Curr. Med. Chem*., 2003, **10**, 1563-1572.

(6) K. Maaser, P. Grabowski, A.P. Sutter, M. Höpfner, H.D. Foss, H. Stein, G. Berger, M. Gavish, M. Zeitz, H. Scherübl, *Clin. Cancer Res.,* 2002, **8**, 3205-3209.

(7) L. Veenman, E. Levin, G. Weisinger, S. Leschiner, I. Spanier, S.H. Snyder, A. Weizman, M. Gavish, *Biochem. Pharmacol.,* 2004, **68**, 689-698.

(8) V. Laquintana, N. Denora, T. Musacchio, M. Lasorsa, A. Latrofa, G. Trapani, *J. Control. Release,* 2009, **137**, 185**–**195.

(9) N. Denora, V. Laquintana, A. Trapani, H. Suzuki, M. Sawada, G. Trapani, *Pharm. Res.,* 2011, **28**, 2820-2832.

(10) N. Denora, V. Laquintana, A. Trapani, A. Lopedota, A. Latrofa, J.M. Gallo, G. Trapani, *Mol. Pharm*., 2010, **7**, 2255**–**2269.

(11) N. Denora, V. Laquintana, A. Lopalco, R. M. Iacobazzi, A. Lopedota, A. Cutrignelli, G. Iacobellis, C. Annese, M. Cascione, S. Leporatti, M. Franco, *J. Control. Release,* 2013, **172**, 1111-1125.

(12) N. Margiotta, R. Ostuni, R. Ranaldo, N. Denora, V. Laquintana, G. Trapani, G. Liso, G. Natile, *J. Med. Chem*., 2007, **50**, 1019**–**1027.

(13) N. Margiotta, N. Denora, R. Ostuni, V. Laquintana, A. Anderson, S.W. Johnson, G. Trapani, G. Natile, *J. Med. Chem*., 201**0**, **53**, 5144**–**5154.

(14) G. Trapani, V. Laquintana, N. Denora, A. Trapani, A. Lopedota, A. Latrofa, M. Franco, M. Serra, M.G. Pisu, I. Floris, E. Sanna, G. Biggio, G. Liso, *J. Med. Chem.,* 2005, **48**, 292-305.

(15) N. Denora, V. Laquintana, M.G. Pisu, R. Dore, L. Murru, A. Latrofa, G. Trapani, E. Sanna, *J. Med. Chem.,* 2008, **51***,* 6876-6888.

(16) A.M. Scarf, L.M. Ittner, M. Kassiou, *J. Med. Chem.,* 2009, **52**, 581-592.

(17) A. Cappelli, A. Mancini, F. Sudati, S. Valenti, M. Anzini, S. Belloli, R.M. Moresco, M. Matarrese, M. Vaghi, A. Fabro, F. Fazio, S. Vomero, *Bioconjugate Chem.,* 2008, **19**, 1143-1153.

(18) S. Piccinonna, N. Margiotta, N. Denora, R.M. Iacobazzi, C. Pacifico, G. Trapani, G. Natile, *Dalton Trans.,* 2013, **42**, 10112-11015.

(19) S. Piccinonna, N. Denora, N. Margiotta, V. Laquintana, G. Trapani, G. Natile, *Z. Anorg. Allg. Chem.,* 2013, **639**, 1606-1612.

(20) N. Denora, N. Margiotta, V. Laquintana, A. Lopedota, A. Cutrignelli, M. Losacco, M. Franco, G. Natile, *ACS Med. Chem. Lett.,* 2014, **5**, 685-689.

(21) S. Liu, *Chem. Soc. Rev.,* 2004, **33**, 445–461.

(22) S.Özalp-Yaman, P. de Hoog, G. Amadei, M. Pitié, P. Gamez, J. Dewelle, T. Mijatovic, B. Meunier, R. Kiss, J. Reedijk, *Chem. Eur. J.,* 2008, **14**, 3418-3426.

(23) R. Alberto, *Eur. J. Inorg. Chem.,* 2009, **1**, 21-31.

(24) U. Abram, R. Alberto, *J. Braz. Chem. Soc.,* 2006, **17**, 1486-1500.

(25) L.S. Hollis, A.R. Amundsen, E.W. Stern, *J Med Chem.,* 1989, **32**, 128–136.

(26) G.Y. Park, J.J. Wilson, Y. Song, S.J. Lippard, *Proc. Natl. Acad. Sci. USA*., 2012, **109**, 11987–11992.

(27) K.S. Lovejoy, R.C. Todd, S. Zhang, M.S. McCormick, J.A. D'Aquino, J.T. Reardon, A. Sancar, K.M. Giacomini, S.J. Lippard, *Proc. Natl. Acad. Sci. USA*, 2008, **105**, 8902–8907.

(28) S. Zhang, K.S. Lovejoy, J.E. Shima, L.L. Lagpacan, Y. Shu, A. Lapuk, Y. Chen, T. Komori, J.W. Gray, X. Chen, S.J. Lippard, K.M. Giacomini, *Cancer Res.,* 2006, **66**, 8847–8857.

(29) R. Alberto, A. Egli, U. Abraham, K. Hegetschweiler, V. Gramlich, P.A. Schubiger, *J. Chem. Soc., Dalton Trans.,* 1994, **19**, 2815–2820.

(30) N. Lazarova, S. James, J. Babich, J. Zubieta, *Inorg. Chem. Commun.,* 2004, **7**, 1023–1026.

(31) M. Bartholomä, J. Valliant, K.P. Maresca, J. Babich, J. Zubieta, *Chem. Commun*., 2009, 493-512.

(32) C. Moura, L. Gano, I.C. Santos, I. Santos, A. Paulo, *Eur. J. Inorg. Chem*., 2011, 5405-5413.

(33) H.W. N'Dongo, P.D. Raposinho, C. Fernandes, I. Santos. D. Can, P. Schmutz, B. Spingler, R. Alberto, *Nucl. Med. Biol*., 2010, **37**, 255-264.

(34) Y. Liu, B. Spingler, P. Schmutz, R. Alberto, *J. Am. Chem. Soc*., 2008, **130**, 1554-1555.

(35) R. Alberto, R. Schibli, P.A. Schubiger, U. Abram, H.J. Pietzsch, B. Johannson, *J. Am. Chem. Soc*., 1999, **121**, 6076-6077.

(36) C. Bolzati, D. Carta, N. Salvarese, F. Refosco, *Anticancer Agents Med. Chem*., 2012, **12**, 428-461.

(37) C.R. Barone, M. Benedetti, V.M. Vecchio, F.P. Fanizzi, L. Maresca, G. Natile, *Dalton Trans*., 2008, **39**, 5313–5322.

(38) D.S. Wishart, C.G. Bigam, J. Yoo, F. Abilgaard, H.J. Dyson, E. Oldfield, J.L. Markley, B.D. Sykes, *J. Biomol. NMR,* **1995**, **6**, 135-140.

(39) H. Miettinen, J. Kononen, H. Haapasalo, P. Helén, P. Sallinen, T. Harjuntausta, H. Helin, H. Alho, *Cancer Res.,* 1995, **55**, 2691-2695.

(40) J. P. Maquet, J. –L. Butour, *J. Natl. Cancer Inst.,* **1983**, *70*, 899-905.

(41) L.R. Kelland, G. Abel, M.J. McKeage, M. Jones, P.M. Goddard, M. Valenti, B.A. Murrer, K.R. Harrap, *Cancer Res.,* 1993, **53**, 2581-2586.

(42) D. Wang, S.J. Lippard, *Nat. Rev. Drug Discov.,* 2005, **4**, 307-320.

(43) K. Datta, P. Shah, T. Srivastava, S.G. Mathur, P. Chattopadhyay, S. Sinha, *Cancer Gene Therapy*, 2004, **11**, 525-531.

Table of Contents

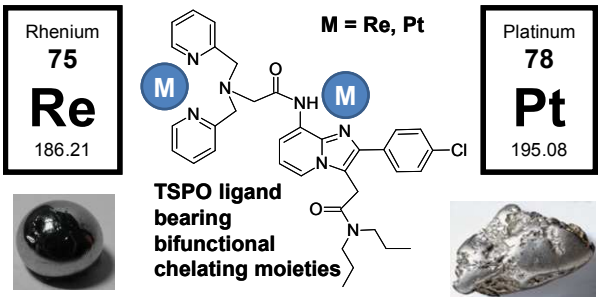

Rhenium
75
Re
186.21

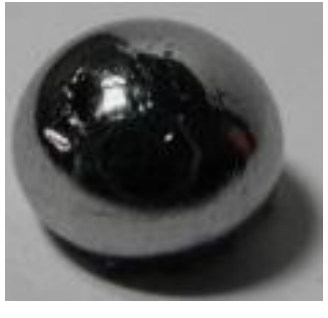

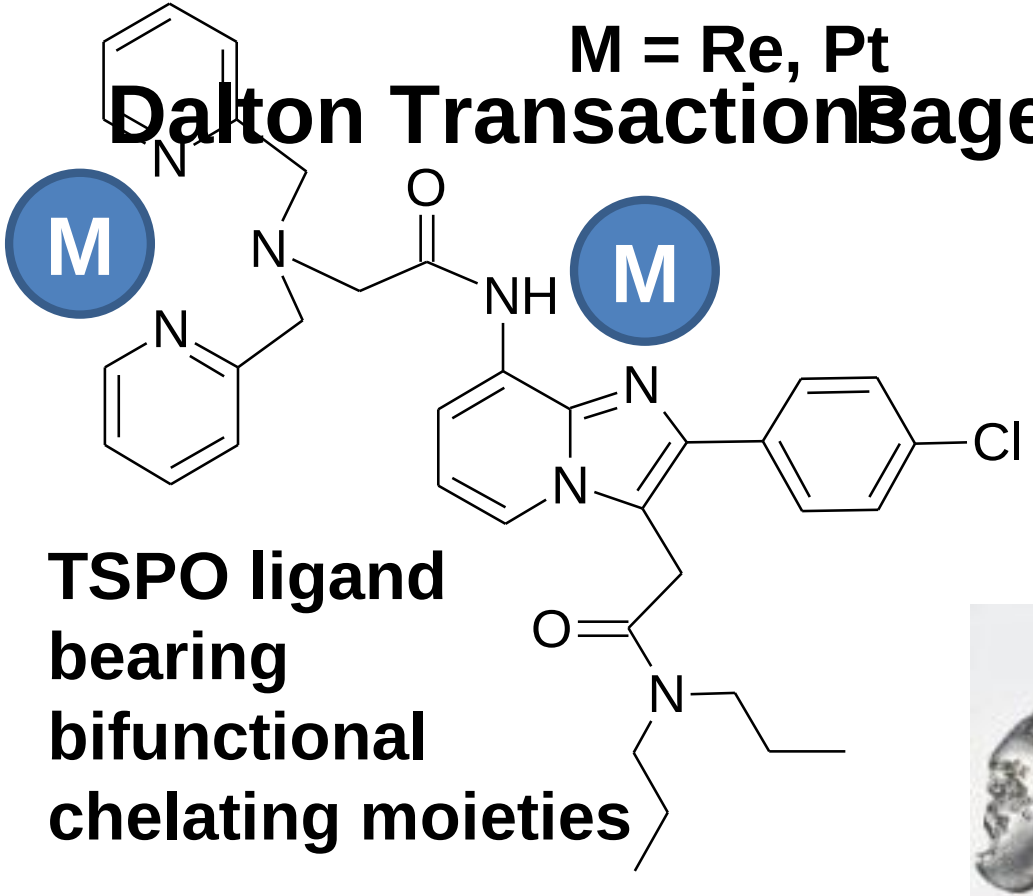

TSPO ligand bearing bifunctional chelating moieties

Platinum
78
Pt
195.08